IOP Publishing Journal of Optics
J. Opt. **16** (2014) 105209 (8pp) doi:10.1088/2040-8978/16/10/105209

Gain broadening and mode-locking in overcoupled second harmonic Q-switched microsecond pulses*

Ingo Rohde[1] **and Ralf Brinkmann**[1,2]

[1] Institute of Biomedical Optics, University of Lübeck, Lübeck, Germany
[2] Medical Laser Center Lübeck, Lübeck, Germany

E-mail: rohde@bmo.uni-luebeck.de

Received 1 April 2014, revised 19 May 2014
Accepted for publication 29 May 2014
Published 3 October 2014

Abstract
An intracavity frequency doubled, Q-switched Nd:YLF emitting at a wavelength of 527 nm was designed with the goal to temporally stretch the Q-switched pulses up to some microseconds at pulse energies of several millijoules. With different resonator configurations pulse durations between 12 μs and 3 μs with energies of 1 mJ–4.5 mJ have been achieved, which is demanded for an application in ophthalmology. For tighter intracavity foci and high pump power, however, strong power modulations by trains of picosecond pulses on the rear flank of the microsecond pulses were observed, indicating the occurrence of cascading nonlinearities and mode-locking. Simultaneously a significant increase of the fundamental spectrum up to 5 nm was found. A similar effect, which is referred to as gain broadening, has previously been observed by using ppKTP for intracavity second harmonic generation. This is, to the best of our knowledge, the first observation of this effect with unpoled second harmonic media.

Keywords: intracavity second harmonic generation, overcoupling, Q-switch, gain broadening, mode-locking
PACS numbers: 42.65.Ky, frequency conversion, harmonic generation, including higher-order harmonic generation

(Some figures may appear in colour only in the online journal)

1. Introduction

For many applications of pulsed lasers such as material processing, short pulses with high peak power are suitable. However, for some applications it is required to limit the peak power in order to avoid laser induced optical breakdown e.g. to prevent damage on optics and coatings, in spontaneous Raman-scattering spectroscopy or to save the tips of optical fibres [1, 2], while still a high pulse energy is required. In these cases, often a temporally stretched Q-switched pulse can be used. An example from the medical field is laser lithotripsy where pulse energies >20 mJ are needed while the intensity damage threshold of multimode quartz fibres shall not be exceeded. For this application a flashlamp pumped, Q-switched Alexandrite laser system was developed, frequency doubled to near UV and pulse stretched by an electronic feedback device from 200 ns to 1 μs. This allowed 25 mJ laser pulses at 1 μs to be transmitted via optical fibres [3].

Another current application is the selective retina therapy (SRT), which requires a train of 30 pulses in the green spectral range with a repetition rate of 100 Hz, a pulse duration of 1.7 μs and pulse energies up to several millijoules, depending on the chosen retinal spot size [4]. These parameters minimize thermal and mechanical stress by adapting the pulse duration to stay within the thermal confinement of the heated tissue, reducing heating of adjacent tissue and by avoiding the acoustic confinement which would lead to explosive microvaporization [5–9].

* This project was realized with the support of the German Ministry for Education and Research (BMBF).

In order to realize the parameters required for SRT, an arc-lamp pumped, Q-switched and intra cavity frequency doubled Nd:YLF laser system was realized, in which the pulses were stretched up to 3 μs by controlling the round trip losses via an electronic feedback loop acting on a pockels cell [6]. However, this process is complex since it needs to control the voltage on the pockels cells in the order of 1 kV within about 10 ns in order to modify intracavity losses during the Q-switched pulse.

Another approach to generate extended Q-switched pulses from few nanoseconds into the microsecond time regime was firstly proposed in 1970 by Murray and Harris [10], using intracavity second harmonic generation (SHG) in the overcoupling regime. The principle of SHG overcoupling is based on the fact that the nonlinear crystal inside the cavity acts as a variable output coupler due to the nonlinear power conversion from the fundamental wave to the second harmonic. The peak power is reached when the linear and nonlinear losses equal the gain for the fundamental mode. In case of high conversion efficiency the inversion population is not much depleted at this point in time. As a consequence, the stored remaining energy is slowly depleted in an extended pulse with a long exponentially decreasing rear flank. In this so called overcoupling regime the pulse energy only decreases slightly with increasing conversion efficiency while the pulse duration increases significantly. Thus the overcoupling effect provides a method to adjust the pulse duration without significant loss of energy [11–13]. Generation of microsecond pulses with durations of 3.2 μs at 3.4 mJ by utilizing this technique has been demonstrated at a wavelength of 527 nm [11].

The aim of this work covers two parts: the first is the development of a compact laser system capable of emitting green microsecond pulses in the millijoule energy regime at a repetition rate of 100 Hz in order to allow further biomedical investigations.

For this, a compact, longitudinally pumped and two times folded resonator with intracavity SHG for use of the overcoupling effect was designed and investigated. Additionally, the use of a quasi cw pump source is explored allowing better heat management at the low repetition rate of 100 Hz.

The second aim is the investigation of the overcoupling effect itself with respect to further increase of the pulse energy and pulse duration as well as the limitations of this method.

2. Material and method

2.1. Background

2.1.1. Overcoupled SHG. In order to illustrate the overall behaviour of the overcoupling effect with regard to pulse energy and duration in dependence of the nonlinear coupling, a set of rate equations for intracavity SHG in plane-wave, fixed-field approximation according to [11] has been implemented and solved. The estimations follow the approach in [14] with a term for the round trip losses extended by a contribution of the nonlinear single pass loss factor $\gamma_{\mathrm{NL}}(t)$ of the resonator taking the nonlinear saturation of the conversion into account. The rate equations for the inversion density $n(t)$ and the laser intensity $I(t)$ are:

$$\frac{\mathrm{d}n(t)}{\mathrm{d}t} = -\frac{\sigma_{\mathrm{SE}}}{h\nu} n(t) I(t) \tag{1}$$

$$\frac{\mathrm{d}I(t)}{\mathrm{d}t} = \frac{2\sigma_{\mathrm{SE}} l}{\tau_{\mathrm{R}}} n(t) I(t) - \frac{1}{\tau_{\mathrm{R}}} \left(\ln\left(1 - \gamma_{\mathrm{L}}\right) + 2\ln\left(1 - \gamma_{\mathrm{NL}}(t)\right) \right) I(t) \tag{2}$$

with the photon round trip time inside the resonator τ_{R}, the linear round trip losses γ_{L} and the cross-section for stimulated emission σ_{SE}. The nonlinear losses $\gamma_{\mathrm{NL}}(t)$ and the nonlinear coupling β are defined as:

$$\gamma_{\mathrm{NL}}(t) = \frac{P_{2\omega}(t)}{P_{\omega}(t)} = \tanh^2\left[\beta\sqrt{\frac{P_{\omega}(t)}{A}}\right] \tag{3}$$

and

$$\beta = \sqrt{2\eta^3}\, d_{\mathrm{eff}}\, l\omega_F \frac{\sin \Delta k l/2}{\Delta k l/2} \tag{4}$$

The conversion $P_{2\omega}(t)/P_{\omega}(t)$ from the fundamental frequency ω to the second harmonic 2ω primarily depends on the nonlinear crystal parameters as the length l and its effective nonlinear coefficient d_{eff} as well as the fundamental beam area A therein. Furthermore, $\eta = 377/\eta_0$ is the plane wave impedance with the refractive index η_0 of the nonlinear crystal and $\Delta k = \frac{4\pi}{\lambda_1}(n_1 - n_2)$ is the phase mismatch.

Figure 1 shows an exemplary evaluation of the dependence of the pulse energy and duration on the nonlinear coupling β with $\Delta k = 0$, thus under perfect phase matching conditions. The parameters were adapted to the setup used here with Nd:YLF as active medium and KTP as a nonlinear crystal as further described below. The parameters used for the calculations are $\lambda = 1053$ nm for the wavelength, an effective cross-section $\sigma_{\mathrm{SE}} = 1.2 \times 10^{-19}$ cm^2, a fluorescence life time $\tau = 480\,\mu$s, a resonator length of $l_{\mathrm{R}} = 60$ cm, linear losses of $\gamma_{\mathrm{L}} = 0.06$ and $d_{\mathrm{eff}} = 27.72 \times 10^{-24}$ As/V^2. A mean diameter of $d_{\mathrm{L}} = 1.5$ mm with a length of $l = 50$ mm was assumed for the active volume inside the laser crystal. This gives a start inversion of $n_i = 7.3 \times 10^{17}$ cm^{-3} assuming homogeneous excitation at a pump power of $P = 40$ W, provided that 80% of the pump power is absorbed.

With increasing nonlinear coupling, the pulse energy increases up to 7 mJ and a pulse duration of some nanoseconds at a conversion factor of $\beta = 1.4 \times 10^{-3}$ mm W$^{-1/2}$ exhibiting the maximal extractable output energy in this example. With increase of β the stays constant, but the pulse duration rises. Exceeding $\beta = 5 \times 10^{-3}$ mm W$^{-1/2}$, the pulse energy drops while the pulse duration grows up to several microseconds.

2.1.2. Nonlinear mirror mode-locking (NLM). A special application of intracavity SHG is the NLM technique, which is used to generate passively mode-locked pulses. It was first reported by Stankov *et al* in 1989 [15] and since that time it was further investigated by various groups [16–20].

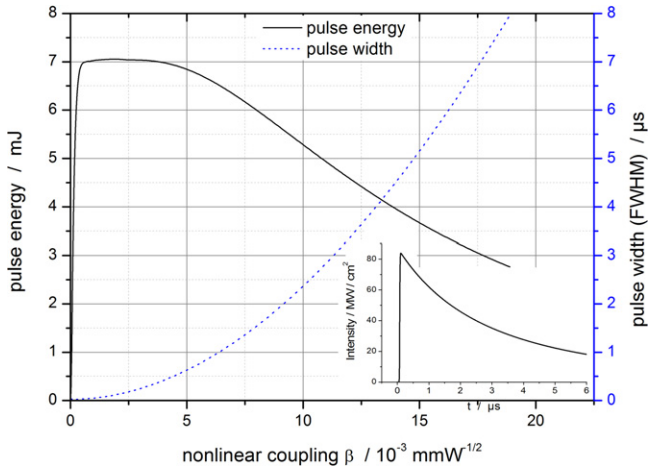

Figure 1. Second harmonic pulse energy and duration in dependence of the conversion factor k in a plane wave, fixed field simulation. The inset shows a typical SHG pulse shape with the approximation parameters as given in the text at a nonlinear coupling of $\beta = 9.5 \times 10^{-3}$ mmW$^{-1/2}$. The intensity refers to a focal radius of 200 μm at the SHG crystal. The pulse energy is 5.5 mJ at a pulse width of 2.25 μs FWHM.

Typical NLM consists of an intracavity SHG crystal placed near a dichroitic mirror which is used as a partial reflective output coupler for the fundamental wavelength and as a high reflector for the second harmonic. In this way, the SH with the correct phase shift, is reconverted into the fundamental wavelength at the second pass through the nonlinear crystal.

For low intensities, the generated second harmonic is negligible and the reflectivity is determined by the dichroitic mirror and the second harmonic losses. For high intensities on the other hand the conversion into the second harmonic rises and enables the back conversion into the fundamental leading to an effective higher reflectivity of the system for the fundamental wavelength [15]. Therefore, the combination of the nonlinear crystal and the dichroitic mirror behaves as a nonlinear mirror with an intensity dependent reflection coefficient, where the laser losses decrease with increasing intensity thus acting as a saturable absorber [21].

Since SHG is a second order nonlinear optical process, as well as the reverse conversion process, that process is associated with a class of interactions referred to as multistep or cascaded second order nonlinearities which can initiate higher order nonlinear optical processes such as four wave mixing, Kerr lensing or the generation of higher harmonics [22].

2.2. Laser setup

2.2.1. Laser crystal. Nd:YLF was chosen as laser material because of its low differential cross-section of stimulated emission of 1.2×10^{-19} cm^2 at a wavelength of 1053 nm and its weak thermal lensing. Additionally, the long fluorescence lifetime of about 480–520 μs allowed longer pump pulses at a reduced pump power while maintaining the overall pump energy in Q-switched mode [14]. The laser crystal was a c-cut Nd:YLF with a length of 50 mm at a diameter of 4 mm and a dopant level of 0.5% (GWU, Germany). It was conduction cooled by a water chilled copper block. A negative thermal lens was measured via resonator stability and ranges from −19 m at a pump power of 36 W over −4 m at 80 W up to −2.5 m at 115 W.

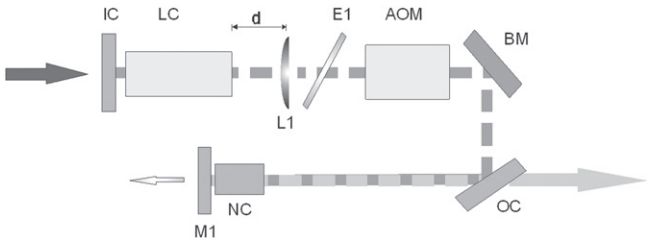

Figure 2. Sketch of the resonator setup. The distance d between the laser crystal LC and the intracavity lens L1 was varied between 10 to 50 mm. The arrows denote the pump beam (top left), SHG output (right) and leakage through end mirror M1 (bottom left) used for measurements of the fundamental wave.

2.2.2. Pump source. A longitudinal laser pumping geometry was chosen. As pump source a fibre coupled 100 W diode laser operated at a wavelength of 805 nm was used (HLU100FQ-800-806, Limo, Germany). The pump pulse duration was set to 500 μs at a repetition rate of 100 Hz. Detuning the pump wavelength from the crystals absorption peaks at 792 and 797 nm [23, 24] in combination with the low dopant level allowed to minimize temperature induced mechanical stress as well as energy upconversion [25]. The fibre core diameter is 800 μm with $N_A = 0.22$. The pump radiation was collimated by a planoconvex lens with a focal length of $f = 25$ mm and focussed into the laser crystal by a second planoconvex lens with $f = 40$ mm (Edmund Optics, USA). This produced a focus of approx. 1.3 mm diameter 25 mm inside the laser crystal. The spot size at entry of the laser rod was about 2 mm in diameter.

2.2.3. Resonator. The resonator was built with a plane input coupler IC (Layertec, Germany) followed by the YLF laser crystal LC at a distance of 2–3 mm as shown in figure 2. Behind this, an intracavity planoconvex lens L1 with a focal length of $f = 500$ mm (LPX 319/126, MellesGriot, USA) was placed on a rail and could be moved over a distance d of several centimetres in order to adjust the focus diameter.

If necessary, an uncoated etalon E1 (Hellma Optik, Germany) was inserted behind the lens. At a thickness of 0.5 mm and a refractive index $n = 1.45$, the free spectral range was about 0.76 nm with a minimum transmission of $T = 0.87$ and a finesse of 0.6.

A 57° brewster mirror BM (CVI Laser Optics, USA) for polarization control, an acousto-optic modulator (AOM, Gooch and Housego, GB) for Q-switching, a dichroitic mirror OC (Layertec, Germany), a nonlinear crystal NC for intracavity SHG and an end mirror M1 (Layertec, Germany) with high reflectivity for both, the fundamental and the second harmonic wavelengths were used. The typical resonator length was 61 cm in combination with a focal length of $f = 500$ mm of the lens. For comparison a lens with $f = 300$ mm at a resonator length of 39 cm has also been used.

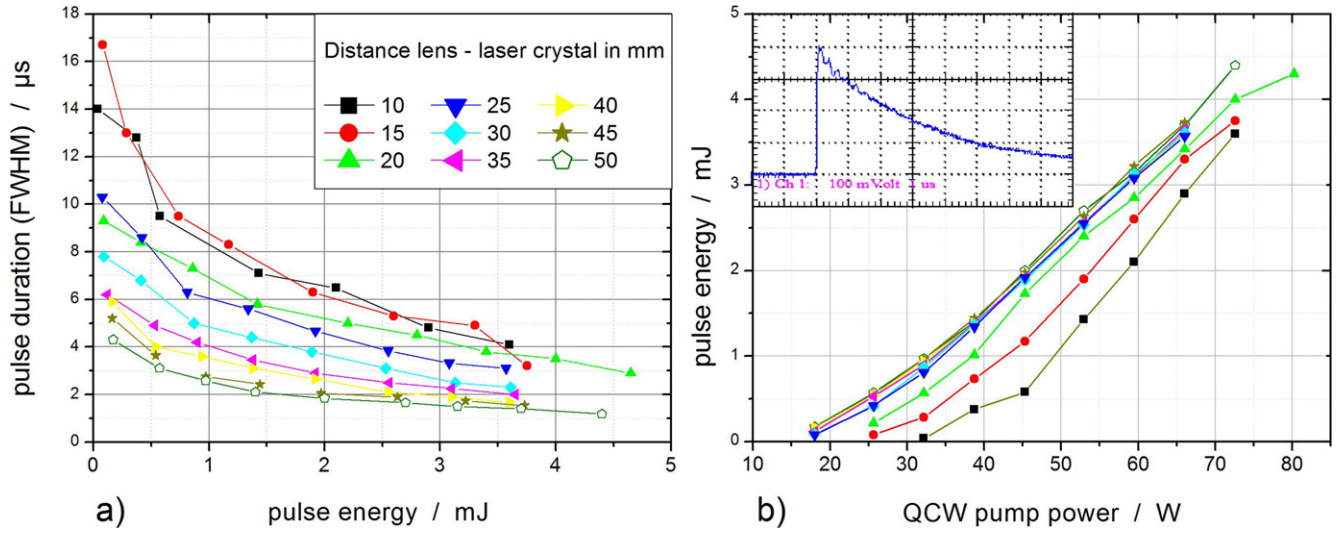

Figure 3. Combinations of pulse durations and energies for different lens positions with a KTP crystal of 14 mm in length. (a) shows the SHG pulse duration versus the pulse energy, (b) the pulse energy in dependence of the pump power. The inset displays a typical pulse trace with a width of approx. 2.4 μs FWHM (1 μs div^{-1}).

In order to analyse the beam radius inside the resonator, calculations with the software WINLASE (Winlase, USA) has been performed. The TEM_{00} radius for the fundamental wavelength of 1053 nm was calculated for three different lens positions with a thermal lens of $f = -4$ m which corresponds to a medium pump power of 80 W as described before. For a distance $d = 50$ mm between the laser crystal and the lens, the beam radius inside the laser crystal was about 0.64 mm with a focal radius of 0.28 mm at the SHG crystal. At $d = 30$ mm the radius at the laser crystal increased to 0.7 mm whereas the focus decreased to 0.26 mm and with $d = 10$ mm the radius was 0.78 mm with a focus of 0.24 mm.

2.2.4. SHG crystal. For frequency conversion a type II KTP crystal ($\theta = 90°$, $\phi = 32.8°$, GWU, Germany) with an aperture of 4×4 mm^2 and a length of 14 mm has been used because of the high nonlinear coefficient $d_{eff} = 3.13$ pm V^{-1} combined with a high damage threshold of 0.5 GW cm^{-2}. The acceptance bandwidths are 28.6 K cm for temperature, 0.56 nm cm for the spectral line width and 9.1 mrad cm for beam divergence. The walk-off is 5.1 mrad [26].

2.3. Laser measurements

2.3.1. Power and pulse shape. The pulse energies were measured with an energy meter in combination with a sensor head (Laserstar and PE10, Ophir, Israel). The low resolution pulse shapes were recorded with a FND 100 photodiode (Laser Components, Germany) and an oscilloscope (TDS 220, Tektronix, USA). Additionally, for the high resolution measurements a photodiode with 12 GHz bandwidth (AR-S1, Antel Optronics, USA) and an oscilloscope with 6 GHz bandwidth (DPO 70604, Tektronix, USA) were used.

2.3.2. Spectral measurements. In order to investigate the spectral behaviour, a high resolution spectrum analyser (AQ6319, Yokogawa, Japan) has been used. The spectral range only allowed the observation of the fundamental wavelengths. Furthermore, the analyser could not be synchronized to the laser repetition rate. Therefore the integration time was chosen to cover a fixed number of pulses for each wavelength interval, before switching to the next. As such, the spectrum of a single pulse could not be recorded.

3. Results

3.1. Microsecond pulses: stable regime

Figure 3 shows the achieved pulse durations in dependence of the pulse energies for different intracavity lens positions and thus different focus parameters measured with a 14 mm KTP. The values in the legend designate the distance d between the laser rod and the intracavity lens in millimetres, therefore the fundamental beam is focussed more tightly for decreased values. This nomenclature is used because the actual beam diameters change with thermal lensing for different pump powers as well as the lens position.

For all the distances investigated, the pulse durations decrease with increasing pump power, which is due to the exponentially growing gain at increased pulse energies, which cannot be compensated by the overcoupling effect in the same manner. Additionally, the negative thermal lens of Nd:YLF broadens the focus with increased pump power, thus decreasing the SHG efficiency.

In direct comparison, the pulse durations increase with decreasing distances d because of the tighter foci and therefore higher conversion efficiencies. For example, the pulse durations at pulse energies around 2 mJ start at 2 μs at $d = 50$ mm and rise up to 6 μs for distances d of 10 and 15 mm.

The pulse parameters presented this far can be generated reliably, once the laser system is in thermal equilibrium. An increase in pump power, exceeding 73 W and pulse energies of

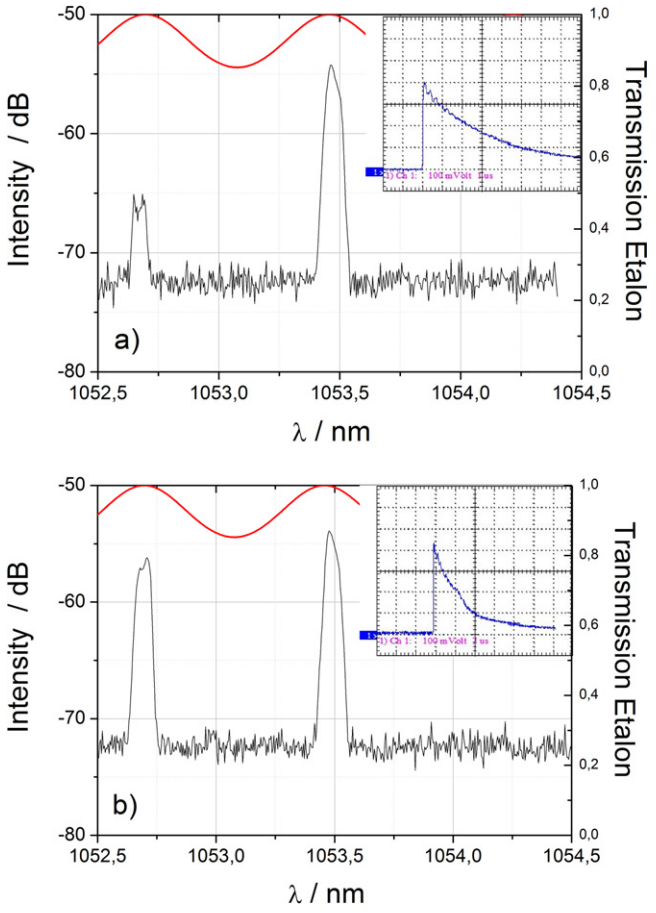

Figure 4. SH pulse shapes and high resolution spectra of the fundamental wavelength. (a) stable (b) instable, both with etalon at 3.6 mJ. The insets represent the according pulse traces with scales of 1 μs div^{-1} (a) and 2 μs div^{-1} (b). For illustration, the calculated transmission curve of the etalon with a minimum transmission of T = 0.87 is also shown.

3.6–4.4 mJ however, lead to irregular pulse shapes and spiking, often accompanied by damages of the antireflection coatings, which can hardly be explained by the theory of overcoupling.

3.2. Instabilities: gain broadening

Figure 4 shows the second harmonic pulse shapes and the spectra at the fundamental wavelength of two sample pulses stabilized with an uncoated quartz etalon with a thickness of 0.5 mm. Figure 4(a) shows a stable pulse of 3.6 mJ with the typical pulse shape of an overcoupled pulse at a FWHM pulse duration of 2 μs. The corresponding spectrum displays a central peak wavelength at 1053.4 nm as well as a small satellite at 1052.7 nm, but with a significantly lower intensity. Figure 4(b) shows the results with slightly increased pump power. While the measured second harmonic pulse energy doesn't change, the pulse shape displays a small irregularity at the falling slope after 2 μs. In addition, relative intensities of the central and satellite peaks in the corresponding spectrum exhibit a significant increase at the wavelength of 1052.7 nm. In both cases, the satellites arise at a neighbouring transmission maximum of the etalon.

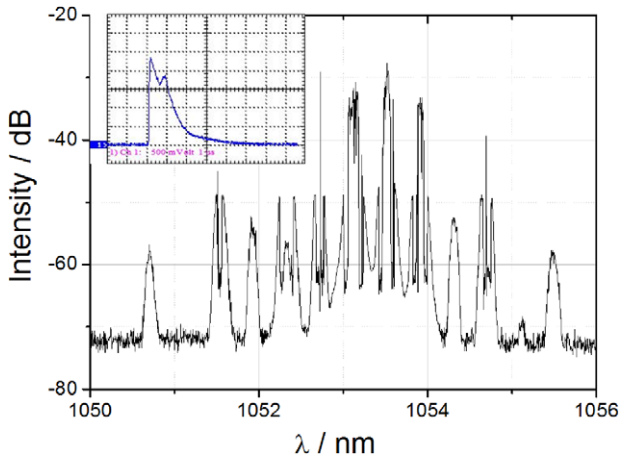

Figure 5. SH pulse shape (1 μs div^{-1}) and high resolution spectrum of the fundamental wavelength of a pulse not been stabilized with an etalon.

Figure 5 shows a pulse of 1 mJ without the use of the etalon. In this case, the SH pulse shape shows a double peak at a pulse duration of 1.1 μs. More significantly, the fundamental spectrum shows a multiplet of different peaks ranging from 1050.7 nm to 1055.5 nm with three peaks of highest intensity between 1053 and 1054 nm.

3.3. Instabilities: nonlinear mode-locking

In order to further investigate the peculiar changes of the pulse shapes coincidencing with the pulse fluctuations, high resolution transients of the second harmonic pulses are recorded. In this set of data an intracavity lens with $f = 300$ mm at a resonator length of 39 cm was used.

Figure 6(a) displays the high resolution trace as recorded with a 6 GHz oscilloscope, clearly showing spikes on the falling slope of the pulse. The detailed view of this regime in figure 6(b) shows repetitive sub pulses of 245 ps FWHM. The constant repetition time of 3 ns, which matches well the round trip time of this setup, indicates a mode-locking process. For comparison, low resolution traces of the second harmonic (figure 6(c)) and the fundamental pulse (figure 6(d)) are also shown. While the former hardly shows an aberration from the stable pulse shape, the latter shows a broad maximum, which exceeds the first maximum at the rising edge of the pulse and thus a completely different pulse shape than its SH pulse.

4. Discussion

4.1. Stable regime

We designed a longitudinally diode pumped, Q-switched Nd:YLF laser system for efficient operation in the TEM_{00} ground mode with μs pulse durations. For this, a good match between the pump and laser mode was required as well as a very high nonlinear coupling.

With this setup pulse energies >4 mJ with pulse durations >3 μs FWHM and 2.5 mJ with 9 μs FWHM were obtained.

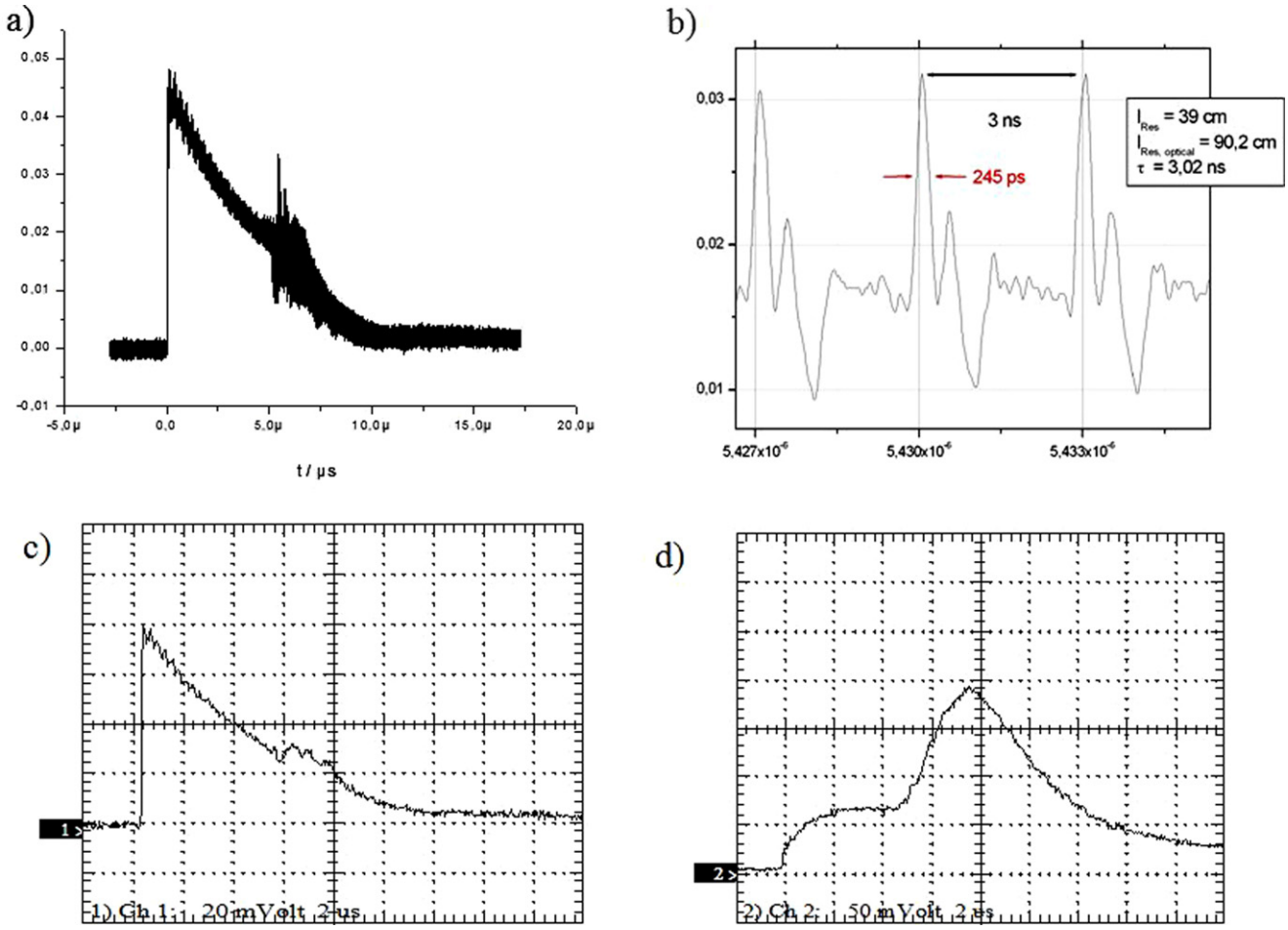

Figure 6. (a) Mode-locking can be observed via high temporal resolution traces of the SH pulse. (b) Shows a cut-out of the spikes on the falling slope, which consists of 245 ps pulses. The repetition time of 3 ns corresponds well to the round trip time of the resonator. (c) Low resolution pulse trace of the second harmonic pulse (2 μs div^{-1}). In this case, the picosecond spikes cannot be resolved correctly. (d) Low resolution fundamental pulse shape (2 μs div^{-1}) related to the same pulse as (c). Here, a significant maximum appears in the time interval of the mode-locked pulses.

The pulse shapes exhibit a fast increase and a long exponential decay as expected and calculated from theory. One possibility to vary the pulse duration can be achieved by using different lengths of SHG crystals, since the nonlinear coupling under perfect phase matching conditions is proportional to the nonlinear crystal length. Another more elegant way without the need to change components is the adjustment of the intracavity focus radius, as shown in figure 3. This can be understood from theory as the focal radius is inversely proportional to the nonlinear coupling. Focal diameter adjustment can be done by moving the intracavity lens allowing for a wide range operating conditions. As demonstrated in figure 3, e.g. at a pulse energy of 2 mJ the pulse duration can be adjusted between 2 and 6.5 μs and stable pulses up to 4.3 mJ at 3.8 μs could be generated with a 14 mm KTP.

These results represent an increase of 19% in pulse duration and 34% in pulse energy compared to 3.2 μs at 3.2 mJ achieved with 71 W of a transversal diode pumped Nd:YLF laser system in combination with a 10 mm KTP as presented in [11]. However, no unstable regime has been reported.

Compared to the simulations shown in figure 1, the expected range of pulse durations and energies could be reached. For example, the nonlinear coupling of a KTP crystal of 14 mm equates to 9.5×10^{-3} mm W$^{-1/2}$ for a 220 μm beam radius inside the SHG crystal under perfect phase matching conditions.

The simulations in this case give 1.8 μs at 5.8 mJ for a pump power of 50 W, compared to 1.6 μs at 4.4 mJ at a pump power of 70 W. Since only a very simple model was used, without special consideration of the phase mismatch, the observation of gain broadening and nonlinear mode-locking suggest the occurrence of additional effects other than linear losses, e.g. by resonator instability, or reduced nonlinear coupling.

4.2. Instable regime

With increasing energy, however, an unstable pulse regime is reached, leading to damages of the coatings. In order to further investigate this effect, one has to take into account the pulse shape of the SH pulse which does not follow the fundamental in the expected manner. High resolution spectra of

the fundamental wavelength show rises at additional wavelengths, even for stable pulses. This indicates further longitudinal modes oscillation building up on the fundamental wavelengths, which are outside the spectral acceptance range of the doubling crystal. The use of an etalon stabilizes the pulses up to energies of several millijoules at a central wavelength of 1053.4 nm, however even there a satellite can be observed at the neighbouring transmission peak of the etalon at 1052.7 nm. With a small increase of the pump power, the satellites intensities increase, and in the low resolution time trace of the pulse a small variation of the pulse shape can be noticed on the falling slope of the pulse.

This becomes more obvious without use of the etalon, where a group of eleven spikes appear at a notably lower pulse energy of 1 mJ. We observed unusual wide spectra extending over a range of up to 5 nm.

A similar effect, a broadened fundamental spectrum in a Nd:YLF ring laser, intracavity frequency doubled by ppKTP at a wavelength of 1321 nm was described in [27]. It is referred to as gain broadening and also coincidences with mode-locking.

In contrast to the aforesaid, in this work unpoled KTP with significant lower conversion efficiency in combination with a higher gain at the 1053 nm Nd:YLF laser line, but in Q-switched mode of operation, was employed in this work.

4.3. Instable regime: NLM

Using a fast GHz measurement system, pulses with a duration of 245 ps FWHM were observed at the falling slope of the microsecond pulse. The repetition time of 3 ns corresponds well to the calculated round trip time of 2.95 ns of the resonator, indicating the occurrence of mode-locking. This behaviour could be observed with different resonator lengths. The modification to a shorter resonator was performed to verify the coincidence of pulse repetition rate and round trip time, thus confirming the occurrence of mode-locking. This set of measurements has been chosen to illustrate this effect because it was not always possible to record all the pulse traces before damage of an optical coating occurred.

The combination of high intensities and high nonlinearities suggest the appearance of nonlinear mode-locking due to cascaded nonlinearities, such as NLM, polarization switched mode-locking or Kerr-lens mode-locking, as has been reported by various groups [16–20].

A question arises, why mode-locking typically appear at the falling slope, and not at the highest intensity. Analysing all observations, the gain broadening seems to appear first, since the SH and fundamental pulse shapes differ already for stable green pulses (not shown here). First of all, a sufficient number of modes need to build up, before enough modes lock to form the typical mode-locked picosecond pulses.

Since the spectral acceptance bandwidth of a 14 mm KTP is 0.4 nm, it seems conceivable that longitudinal modes, which are not frequency doubled by the SHG crystal, build up, provided that the gain for these frequencies and the losses at the central frequencies are high. The first requirement is fulfilled by operating the laser in Q-switched mode, the second by optimizing the intracavity SHG for overcoupling.

Given that, competing fundamental modes combined with nonlinear frequency mixing may lead to the behaviour of a nonlinear mirror. Therefore, NLM, which is connected to sum frequency generation, seems an explanation. Since many of the satellite modes are not coupled out of the resonator by SHG, they can most likely be made responsible for the observed damage of coatings.

For the purpose of deepening the understanding of all the underlying mechanisms, high resolution spectra of both, the second harmonic and the fundamental pulses, should be recorded simultaneously in order to identify frequencies and possible nonlinear processes participating in these mechanisms. Ideally, the spectra should be recorded at an adequate time gate, e.g. by using a pockels cell as a fast shutter, thereby allowing to obtain separate spectra before, during and after the occurrence of mode-locking during the microsecond pulses. Furthermore, a self-evident approach to increase the pulse energy of microsecond pulses in the stable regime of operation is the use of an improved frequency filter, e.g. a partial reflective etalon with increased finesse and broader spectral range.

5. Conclusions

In this work we demonstrated the application of the overcoupling effect to generate intracavity, frequency doubled Q-switched pulses with pulse energies of several millijoules and pulse durations of several microseconds. In a long term stable regime pulses between 4.5 mJ at a duration of 3 μs and 8 μs at 1.1 mJ can be extracted, thus allowing the use of this laser system for biomedical therapies such as SRT. The pulse duration can be adjusted by potentially motor controlled intracavity lens movement, not requiring the exchange of components.

Beyond this stable regime of operation, the occurrence of mode-locking in sections of the falling slope of the microsecond pulses was found. Furthermore, high resolution pulse traces modulated onto the microsecond pulses confirmed the occurrence of mode-locking in sections of the falling slope of the microsecond pulses.

Simultaneously a significant increase in the width of the fundamental spectrum up to 5 nm was found. This gain broadening effect has previously been reported in ppKTP for intracavity SHG [27] and could for the first time be observed in unpoled second harmonic media. Nevertheless, more investigations of the fundamental and second harmonic spectra are necessary to further elucidate the underlying physics.

Acknowledgements

The authors would like to thank Mr Andreas Oelke and Mr Jörg Latzel of Yokogawa Measurement Technologies GmbH for providing an optical spectrum analyser. This project was

supported by the German Ministry for Education and Research (BMBF), Grant No. 13N8302.

References

[1] Rajeev K and Shukla P K 2010 Temporal stretching of laser pulses *Coherence and Ultrashort Pulse Laser Emission* ed F J Duarte *Intech* 205–26

[2] Beyrau F, Weikl M C, Seeger T and Leipertz A 2004 Application of an optical pulse stretcher to coherent anti-stokes Raman spectroscopy *Opt. Lett.* **29**

[3] Brinkmann R and Schoof K 1994 Intracavity frequency doubling of μs alexandrite laser pulses *Proc. SPIE Visible and UV Lasers* **2115** 94–102

[4] Brinkmann R, Roider J and Birngruber R 2006 Selective retina therapy (SRT): a review on methods, techniques, preclinical and first clinical results *Bull. Soc. Belge Ophtalmol.* **302** 51–69

[5] Moorman C M and Hamilton A M 1999 Clinical applications of the micropulse diode laser *Eye* **13** 145–50

[6] Brinkmann R, Hüttmann G, Rögener J, Roider J, Birngruber R and Lin C P 2000 Origin of retinal pigment epithelium cell damage by pulsed laser irradiance in the nanosecond to microsecond time regimen *Lasers Surg. Med.* **27** 451–64

[7] Schuele G, Rumohr M, Huettmann G and Brinkmann R 2005 RPE damage thresholds and mechanisms for laser exposure in the microsecond-to-millisecond time regimen *Invest. Ophthamol. Vis. Sci.* **46** 714–9

[8] Neumann J and Brinkmann R 2008 Self-limited growth of laser-induced vapour bubbles around single microabsorbers *Appl. Phys. Lett.* **93** 033901

[9] Lin C P and Kelly M W 1998 Cavitation and emission around laser-heated microparticles *Appl. Phys. Lett.* **72** 2800–2

[10] Murray J E and Harrys S E 1970 Pulse lengthening via overcoupled internal second-harmonic generation *J. Appl. Phys.* **41** 609–13

[11] Kracht D and Brinkmann R 2004 Green Q-switched microsecond laser pulses by overcoupled intracavity second harmonic generation *Opt. Commun.* **231** 319–24

[12] Rohde I, Theisen-Kunde D and Brinkmann R 2012 Temporally stretched Q-switched pulses in the 2 μm spectral range *Laser Phys. Lett.* **9** 808–13

[13] Ray A, Das S K, Mishra L, Datta P K and Saltiel S M 2009 Nonlinearly coupled, gain-switched Nd:YAG second harmonic laser with variable pulse width *Appl. Opt.* **48** 765–9

[14] Koechner W 1999 *Solid-State Laser Engineering* (Berlin: Springer)

[15] Stankov K A and Jethwa J 1988 A new mode-locking technique using a nonlinear mirror *Opt. Commun.* **66** 41–6

[16] Danailov M B, Cerullo G, Magni V, Segala D and De Silvestri S 1994 Nonlinear mirror mode locking of a cw Nd:YLF laser *Opt. Lett.* **19** 792–4

[17] Chen Y F, Tsai S W and Wang S C 2001 High-power diode-pumped nonlinear mirror mode-locked Nd:YVO4 *Appl. Phys.* B **72** 395–7

[18] Holmgren S J, Pasiskevicius V and Laurell F 2005 Generation of 2.8 ps pulses by mode-locking a Nd:GdVO4 laser with defocusing cascaded Kerr lensing in periodically poled KTP *Opt. Express* **13** 5270–8

[19] DeSalvo R, Hagan D J, Sheik-Bahae M, Stegeman G, Van Stryland E W and Vanherzeele H 1992 Selffocusing and self-defocusing by cascaded second-order effects in KTP *Opt. Lett.* **17** 28–30

[20] Mani A A, Lis D, Caudano Y, Thiry P A and Peremans A 2011 Optimal performances of a mode-locking technique: theoretical and experimental investigations of the frequency-doubling nonlinear mirror *Opt. Comm.* **284** 398–404

[21] Datta P K, Mukhopadhyay S, Das S K, Tartara L, Agnesi A and Degiorgio V 2004 Enhancement of stability and efficiency of a nonlinear mirror mode-locked Nd:YVO4 oscillator by an active Q-switch *Opt. Express* **12** 4041–6

[22] Saltiel S M, Sukhorukov A A and Kivshar Y S 2005 Multistep parametric processes in nonlinear optics *Prog. Opt.* **47** 1–73

[23] Utano R A, Hyslop D A and Allik T H 1990 Diode-array side-pumped Nd:$YLiF_4$ laser *Proc. SPIE 1223 Solid State Lasers* **128**

[24] Sharp E J, Horowitz D J and Miller J E 1973 High-efficiency Nd^{3+}:LiYF4 laser *J. Appl. Phys.* **44** 5399–401

[25] Peng X, Xu L and Asundi A 2005 High-power efficient continuous-wave TEM00 intracavity frequency-doubled diode-pumped Nd:YLF laser *Appl. Opt.* **44** 800–7

[26] Dmitriev V G, Gurzadyan G G and Nikogosyan D N 1999 *Handbook of Nonlinear Optical Crystals* (Berlin: Springer)

[27] Zondy J-J, Camargo F A, Zanon T, Petrov V and Wetter N U 2010 Observation of strong cascaded Kerr-lens dynamics in an optimally-coupled cw intracavity frequency-doubled Nd:YLF ring laser *Opt. Express* **18** 4796–815